

Stopping-cross-section additivity for 1–2-MeV ${}^4\text{He}^+$ in solid oxides*

J. S.-Y. Feng, W. K. Chu, and M.-A. Nicolet

California Institute of Technology, Pasadena, California 91109

(Received 7 February 1974; revised manuscript received 2 May 1974)

The stopping of 1–2-MeV α particles in five solid oxides, MgO, Al_2O_3 , SiO_2 , $\alpha\text{-Fe}_2\text{O}_3$, and Fe_3O_4 , has been investigated by measuring the ratios of the elastically-back-scattered-particle yields from two-layered metal-oxide and metal-metal targets. By applying a self-consistent analytical procedure, it is demonstrated that within the 2% sensitivity of the experiment, there is a unique set of five elemental stopping cross sections that is applicable to the pure metals and their oxides. When the effective stopping cross section of oxygen in these solid oxides is calculated using the reported Mg, Al, Si, and Fe stopping cross sections, the resulting values are systematically (6–22)% lower than the value reported for gaseous O_2 .

I. INTRODUCTION

In their early investigations on the ranges of natural α particles, Bragg and Kleeman found that the stopping power of a compound is approximately given by a linear combination of the stopping powers of the constituent elements.¹ This assumption has been particularly well-tested for natural α -particle ranges in water and organic compounds. More recently, the Baylor group has studied the energy loss of 0.3–2.0-MeV ${}^4\text{He}$ in several gaseous compounds.^{2–4} Their measurements have revealed both a possible physical-state effect in the stopping cross section of carbon² and chemical binding effects in various hydrocarbon gases.³ However, their measurements on several fluorocarbons showed no evidence of any physical-state effects.⁴

Despite the prevalence of solid targets and the increased use of nuclear techniques for solid-state investigations,⁵ there exist few reports of tests of Bragg's rule in solids. In one case, Thompson and Mackintosh reported deviations of up to 10% in SiO_2 .⁶ We have previously described a self-consistent method for testing Bragg's rule in binary alloys in which mixing between the two normally solid elements is easily induced, and we found that within 1% Bragg's rule correctly predicted the energy loss in mixed metal films from 300 keV to 2 MeV.⁷

We now report the results of combining the methods proposed by Feng *et al.*⁸ and Baglin *et al.*⁹ to produce a test that is applicable to stoichiometric solid compounds in which one of the components is not normally a solid. We have applied this to the specific example of 1–2-MeV ${}^4\text{He}$ in stoichiometric binary oxides. This was chosen as representative of an important class of materials that is amenable to study by ion back scattering.

II. ANALYSIS

Stopping-power additivity, or Bragg's rule, is given by the formula

$$\epsilon_{A_mB_n} = m\epsilon_A + n\epsilon_B, \quad (1)$$

where ϵ_A and ϵ_B are the atomic stopping cross sections in elements A and B , respectively, and $\epsilon_{A_mB_n}$ is the molecular stopping cross section in a compound with the chemical formula A_mB_n . The direct test of the validity of Bragg's rule is performed by comparing the molecular and atomic stopping cross sections.

We demonstrate here that the assumption of linear additivity in solids can be examined without reference to the absolute stopping cross section of any element by performing relative measurements. This ensures that the potentially large systematic errors exactly cancel.

We have measured the ratios of the yields of particles elastically back scattered from the interfaces of two-layered targets. For the case of a layer of element A and a layer of element B , this ratio is given by

$$\frac{Y_A}{Y_B} = \frac{\sigma_A/[\epsilon]_A^A}{\sigma_B/[\epsilon]_B^B}, \quad (2)$$

where Y_A is the back-scattering yield due to element A , σ_A is its scattering cross section, and $[\epsilon]_A^A$ is the stopping cross-section factor of element A .⁸ Corrections to this expression are insignificant in all our present measurements and have not been included.⁸

The $[\epsilon]$ factor is defined by

$$[\epsilon]_y^x = \frac{K_x}{|\cos\theta_{in}|} \epsilon_y|_{E_{in}} + \frac{1}{|\cos\theta_{out}|} \epsilon_y|_{E_{out}} \quad (3)$$

where $[\epsilon]_y^x$ is the $[\epsilon]$ factor for scattering from a

nucleus of type x in an energy-loss medium y . θ_{in} and θ_{out} are the incoming and outgoing angles with respect to the normal to the plane of the target and $\epsilon_y|_E$ is the stopping cross section of the stopping medium evaluated at energy E . K_x is the kinematic factor relating the particle energies before and after elastic scattering from x and is given by the equation

$$K_x = \left(\frac{m \cos \theta + (M^2 - m^2 \sin^2 \theta)^{1/2}}{m + M} \right)^2, \quad (4)$$

where m is the mass of the projectile, M is the mass of the scattering center, and θ is the laboratory scattering angle.

For the case of a layer of element A and a layer of the compound $A_m B_n$, it follows from Eq. (2) that the ratio of the yields of the A signals from the interface is

$$\begin{aligned} \frac{Y_A^A}{Y_{A_m B_n}^A} &= \frac{\sigma_A / [\epsilon]_A^A}{m \sigma_A / [\epsilon]_{A_m B_n}^A} \\ &= \frac{(1/m) [\epsilon]_{A_m B_n}^A}{[\epsilon]_A^A}. \end{aligned} \quad (5)$$

Because the $[\epsilon]$ factor is a linear combination of the stopping powers at two energies, and since Bragg's rule is also a linear relationship, it follows that the ratio of the yields can also be expressed as

$$\frac{Y_A^A}{Y_{A_m B_n}^A} \doteq \frac{[\epsilon]_A^A + (n/m) [\epsilon]_B^A}{[\epsilon]_A^A}, \quad (6)$$

where \doteq indicates that Bragg's rule has been assumed. The ratio of the $[\epsilon]$ factors for A and B can now be calculated from the ratio of the A signals using

$$\frac{[\epsilon]_B^A}{[\epsilon]_A^A} \doteq \frac{m}{n} \left(\frac{Y_A^A}{Y_{A_m B_n}^A} - 1 \right). \quad (7)$$

If $(\epsilon|_{E_{in}})/(\epsilon|_{E_{out}})$ is known for A and for B , the ratio of the $[\epsilon]$ factors can be converted to the ratio of the stopping cross sections ϵ_A/ϵ_B by using Eq. (3). This calculation assumes only that the energy dependence of the elemental stopping cross sections can be precisely determined without knowing the absolute value. The ratio ϵ_A/ϵ_B at the incoming particle energy can thus be determined from the ratio of the scattering yields from A and $A_m B_n$.

The ratio of the $[\epsilon]$ factors can also be determined by a direct comparison of scattering yields from layers of pure A and pure B according to

$$\frac{[\epsilon]_A^A}{[\epsilon]_B^A} = \frac{\sigma_A / Y_A}{\sigma_B / Y_B}. \quad (8)$$

When using this equation, we have assumed that

the scattering cross sections are exactly given by the laboratory-frame Rutherford cross section formula.¹⁰

The straight-forward application of this relative test for Bragg's rule requires only two measurements. The ratio ϵ_A/ϵ_B as determined from a comparison of pure A with pure B must be the same as the ratio determined by comparing pure A with $A_m B_n$. If these two ratios are not the same, the assumption of Bragg additivity cannot be valid.

It is difficult to measure the yield ratios necessary to apply Eq. (8) when one of the elements is normally a gas. However, this procedure can readily be used to compare the contributions of a gaseous element to the stopping in several of its solid compounds. Bragg's rule then requires that this contribution must be the same in all of the compounds.

As applied to our specific examples, consisting of Mg, Al, Si, Fe, and their oxides, a determination of the four stopping-cross-section ratios for Al-Mg, Al-Si, Al-Fe, and Al-O are sufficient to determine the allowed stopping-cross-section ratios for all other combinations. The Al-Mg, Al-Si, and Al-Fe ratios would, of course, be determined from samples of the pure metals, while the Al-O ratios would, of necessity, be determined from the Al-Al₂₀₃ yield ratio. The test of Bragg's rule then consists of measuring the Mg-O, Si-O, and Fe-O stopping-cross-section ratios from samples of MgO, SiO₂, Fe₂O₃, and Fe₃O₄. If Bragg's rule is valid, these ratios must be consistent with the first four ratios.

This example constitutes a system of five unknown quantities, the absolute stopping cross sections of the five elements. It is reduced to four unknowns by introducing relative stopping cross sections. There are over ten ways of pairing these four metals with each other and with their oxides. Since Bragg's rule asserts linearity, the yield-ratio measurements from these pairings define at least ten linear relationships between these four unknowns. The existence of a unique solution for this overdetermined system is necessary for the validity of Bragg additivity.

The analytical procedure described here requires four assumptions to establish the existence of a solution to the overdetermined system. The assumption that we believe we are testing is the applicability of Bragg's rule of linear additivity of elemental stopping cross sections to compounds. A second, and presumably safe assumption is that the scattering cross section of back scattered 2-MeV ⁴He ions is given by the Rutherford formula. Third, the conversion from the back-scattering $[\epsilon]$ factors to the stopping cross section at the

incident particle energy assumes that the relative energy dependence of the stopping cross section, without reference to the absolute value, must be known for each element. Finally, the composition of the targets must be known. Although it is possible that two or more of these assumptions may fail simultaneously, producing a cancellation of errors, this is highly improbable. We take self-consistency as evidence that all of these conditions have been fulfilled.

III. EXPERIMENTAL METHOD

A. Facilities

Measurements were performed using the 3-MV accelerator of the Kellogg Radiation Laboratory to produce 2-MeV ${}^4\text{He}^+$ ions at target currents of 30–200 nA. The particles were detected at a mean laboratory scattering angle of 168° by a 25-mm² silicon-surface-barrier detector about 12 cm from the target. Standard pulse-shaping electronics was used in conjunction with a 50-MHz 512-channel pulse-height analyzer. Charge integration was performed on a standard current-to-frequency converter with electronic and mechanical counters. A 300-V charge-stripping potential at the entrance of the target chamber and a 300-V secondary-electron-suppression bias were used to increase the accuracy of the current integration.

Samples were mounted either on a two-axis goniometer or a sample holder with orthogonal translational and azimuthal position control. Samples on single-crystal substrates or with layers suspected of having a preferred crystalline orientation were mounted on the two-axis goniometer. During the measurement the sample was continually rotated around its polar axis while the azimuthal angle was varied from 5° to 7° . This procedure minimizes channeling effects. Untextured polycrystalline samples were measured with stationary targets and with the incident beam at normal incidence.

B. Sample preparation and measurements

The compounds used in this study were chosen from among those that could, *a priori*, be assumed to be stoichiometric. Nevertheless, the composition was not blithely assumed to be known. With one exception, each type of sample was produced in several different ways.

1. Al- Al_2O_3

The Al_2O_3 -on-Al yield ratio was measured using four different thicknesses of anodically formed Al_2O_3 (presumably $\gamma\text{-Al}_2\text{O}_3$). The Al-on- Al_2O_3

yield ratio was measured using samples of Al evaporated onto (0001) $\alpha\text{-Al}_2\text{O}_3$ (single-crystal sapphire), (11 $\bar{2}$ 0) $\alpha\text{-Al}_2\text{O}_3$, and anodized $\gamma\text{-Al}_2\text{O}_3$.

The $\gamma\text{-Al}_2\text{O}_3$ was formed by anodizing commercial Al foil (supplied by the Reynolds Metal Co., Richmond, Va.) in an aqueous solution of $(\text{NH}_4)_2\text{HC}_8\text{H}_5\text{O}_7$ using current densities of less than 10 mA/cm². The stoichiometry of a film produced by this method was checked by Rutherford back scattering on a self-supporting 1500-Å foil and the oxygen-to-aluminum ratio was found to be 1.53 ± 0.05 . The (0001) $\alpha\text{-Al}_2\text{O}_3$ was supplied by Union Carbide and the (11 $\bar{2}$ 0) $\alpha\text{-Al}_2\text{O}_3$ was supplied by Inselek, Inc., Princeton, N. J., as the substrate of epitaxially grown (111) silicon-on-sapphire.

The accuracy of the Al- Al_2O_3 yield ratio also depends on the purity of the Al layer. The purity of the evaporated Al was determined by simultaneously depositing the Al onto carbon and aluminum foil substrates. The back-scattering spectra taken with these samples are shown in Fig. 1. The

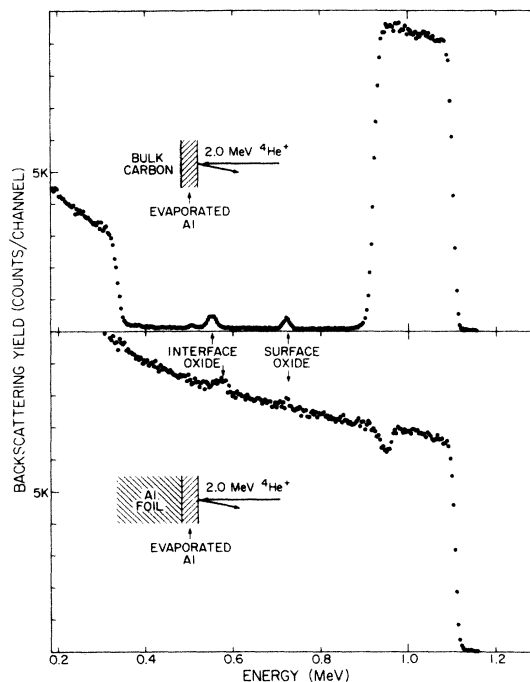


FIG. 1. Purity tests of Al films. The top half of the figure shows a back-scattering spectrum of Al evaporated onto a carbon substrate. This shows the presence of a small amount of oxygen on the two surfaces of the film, but no evidence of bulk impurities. The bottom part shows the spectrum of Al evaporated onto Al foil. The dip in the yield near 975 keV is due to the native oxide on the Al foil. The match in the yields of the evaporated and bulk Al indicates that there are no significant undetected impurities.

Al-on-C spectrum shows evidence of oxidation on both surfaces of the evaporated Al. There are no detectable impurities in the bulk of the evaporated material. The Al-on-Al-foil spectrum shows that the back-scattering yields of the two layers are identical. The dip is due to the native oxide on the Al foil. This shows that there are no significant impurities in the film since the presence of impurities in the evaporated Al would be indicated by a lower back-scattering yield from the deposited layer, just as the interface is marked by the dip due to the oxide on the surface of the foil. The impurity content of the Al foil is assumed to be insignificant.

The Al-Al₂O₃ yield ratios as determined on the seven samples described above was reproducible within better than 1%. The repeatability of the measurements is encouraging evidence both that the method used in this experiment is valid and that the samples are all stoichiometric.

2. Si-SiO₂

The SiO₂-on-Si yield ratio was determined for two different thicknesses of thermally grown SiO₂ on single-crystal Si. The Si-on-SiO₂ ratio was measured for amorphous Si evaporated onto fused quartz, AT-cut quartz, and thermally grown SiO₂.

Thermally grown SiO₂ has been extensively investigated and it is believed that deviations from stoichiometry are below the sensitivity of most experiments. The fused quartz, supplied by Amersil, Inc., Hillside, N. J., is claimed to have less than 100-ppm impurities. The AT-cut single-crystal quartz was removed from an electrically active quartz-crystal resonator.

The purity of the evaporated Si was tested by simultaneously evaporating the Si onto Si and C substrates. Despite a small amount of oxygen contamination of a few percent evident in the Si-on-C sample, the back-scattering yield from the evaporated Si matched the yield from the single crystal to within better than $\pm \frac{1}{2}\%$. The single-crystal silicon is assumed to be pure.

The ratio of the yields from the Si and SiO₂ layers was reproducible within $\pm \frac{1}{2}\%$ for all of these samples.

3. Fe-Fe₂O₃-Fe₃O₄

The composition of the two iron oxides was inferred from the magnetic, electrical, optical, and crystallographic properties. The sample-preparation techniques and the verification of the properties of the oxides have been described elsewhere.⁷

The purity of the Fe films was established by depositing Fe onto a carbon substrate and using back scattering to show no detectable impurities.

Measurements using x-ray fluorescence also showed no evidence of similar mass impurities such as Ni or Co.

The reproducibility of the Fe-Fe₂O₃ and Fe-Fe₃O₄ ratios was better than $\pm 1\%$. The two ratios are also consistent with each other within $\pm 1\%$.

4. Mg-MgO

The Mg-MgO ratio was determined for only one sample. The MgO is a single-crystal (100) wafer supplied by Semi-Elements, Saxonburg, Pa. The Mg film was evaporated from material of better than 99.9% purity in a vacuum of better than 10⁻⁶ Torr. The purity of the Mg films produced this way was not extensively tested, but there was no evidence of any significant impurities in any of the back-scattering spectra.

5. Al-Si

The Al on Si yield ratio was measured for evaporated Al on single-crystal (111) Si and on evaporated Si on a carbon substrate. The Si-on-Al ratio was determined using samples of evaporated Si on Al-foil and evaporated Al. The measured ratios were within $\pm 1\%$ for all samples.

6. Fe-Al

The Fe-Al ratio was measured using Fe evaporated onto Al foil and Al evaporated onto a film of Fe on a Si substrate. One sample of each type was measured and the two yield ratios were almost identical.

7. Fe-Si

The Fe-on-Si ratio was measured with two different thicknesses of evaporated Fe on single-crystal (111) Si. No measurements of the Si-on-Fe ratio were performed. The ratio was reproducible to better than $\frac{1}{2}\%$.

8. Al-Mg

The Al-on-Mg ratio was determined from two samples with different thicknesses of evaporated Al on evaporated Mg on MgO substrates. The Mg-on-Al ratio was measured on a single sample of evaporated Mg on evaporated Al on a thermally oxidized Si substrate. The measured ratios were the same within 2%.

IV. RESULTS

A typical spectrum, for a sample of evaporated Al on (0001) α -Al₂O₃, is shown in Fig. 2. The data were taken using a beam current of 150 nA

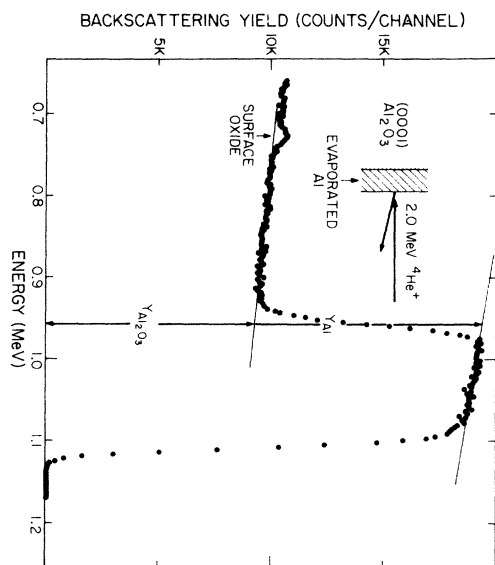


FIG. 2. Yield-ratio measurements. The spectrum was taken by back scattering from evaporated Al on (0001) α - Al_2O_3 . The method of determining the yield ratios by projecting to the interface between the two layers is illustrated.

and a total dose of 500 μC . To avoid anomalous yields due to channeling effects the sample was continually rotated about its polar axis while the azimuthal angle was changed from 5° to 7° in $\frac{1}{2}^\circ$ steps at every 100 μC of incremental dose.

The yield ratio is determined by extrapolating the Al and Al_2O_3 plateaus to the point representing the interface between the two layers and taking the ratio of the projected yields. This procedure ensures that the back-scattered particle yields are evaluated at the same incident-ion energy. Two examples of the extrapolation procedure used for scattering from two dissimilar elements are shown in Ref. 7.

Obviously, the accuracy of the yield-ratio determination does not depend on the accurate measurement of the total ion fluence. This ratio is also relatively insensitive to the scattering geometry and the absolute beam energy because small errors of this type tend to cancel each other when ratios are taken. The effect of the thickness of the surface layer on the yield ratio is negligible.⁸ The only parameters that plausibly affect the determination of this ratio are the composition of the two films, the statistical fluctuations in the data, and the judgment of the investigator in estimating the yield levels.

The results of the yield-ratio measurements are shown in Table I. The number of samples used to determine each ratio and the reproducibility of the experimental ratios are also shown in the table. Since the Mg-MgO yield ratio was mea-

TABLE I. The experimental yield ratios for 168° back scattering of 2-MeV ^4He from two-layered samples. The yield ratio is the yield of the first layer identified in the "sample type" column divided by the yield of the other layer. The standard deviation represents the reproducibility of the measurement. The Mg-MgO ratio was measured only once and the uncertainty is estimated at about 1%.

Sample type	No. of samples	Yield ratio	Standard deviation
Al-Mg	3	1.207	1.8%
Si-Al	4	1.069	0.81%
Fe-Al	2	2.524	0.08%
Fe-Si	2	2.358	0.17%
Mg-MgO	1	1.703	(~1%)
Al- Al_2O_3	7	2.075	0.83%
Si- SiO_2	5	2.356	0.49%
Fe- Fe_2O_3	4	1.678	0.36%
Fe- Fe_3O_4	3	1.616	0.62%

sured on only one sample, the tabulated uncertainty is an estimated value.

The Al-Si, Al-Fe and Fe-Si ratios constitute all possible pairings of Al, Si and Fe. The self-consistency of these is much better than could be expected from uncertainties in each value. This supports the validity of the approach used in this experiment.

The yield ratios from the measurements on the pure metals were used to determine the ratios of the stopping cross sections at 2.0 MeV. Since these are relative values, no absolute values were determined by these measurements. These ratios, normalized to the stopping cross section of silicon, are shown in Table II. Also shown for comparison are the ratios of the stopping cross sections taken from the semiempirical table of Ziegler and Chu.¹¹

The metal-oxide yield ratios were used to determine the ratio of the stopping cross sections of the metal and the oxygen, assuming Bragg's rule. These ratios, calculated for the incident-

TABLE II. Relative α -particle stopping cross sections at 2.0 MeV. The top row identifies the cation in the oxide. The first part shows the results based on our yield-ratio measurements on the pure metals, normalized to Si. Below that are the values found in Ref. 11 (normalized to Si). The bottom row gives the error in the measured ϵ ratio with respect to the values in Ref. 11.

Metal	Mg	Al	Si	Fe
Present				
Measurements	0.985	0.995	1.000	1.485
$\frac{\epsilon_{2.0 \text{ MeV}}}{\epsilon_{\text{cation}}}$				
Ref. 11	0.916	0.898	1.000	1.442
Error	+7.5%	10.8%	...	+3.0%

ion energy of 2.0 MeV, are shown in Table III. In both Tables II and III, the ratios of the $[\epsilon]$ factors were converted to ratios in ϵ by using the semi-empirical values in Ref. 11.

By combining the results of Tables II and III, it is possible to calculate the relative contribution of an oxygen atom to the molecular stopping cross sections of the different oxides. If Bragg's rule is valid, this contribution in one oxide, e.g., Al_2O_3 , must be the same as the contribution in all other oxides. The relative values are shown in Table IV with the estimated error. The values have been normalized to an average value of unity to highlight the consistency of the oxygen stopping cross sections in these five oxides.

Since the absolute stopping cross sections of these five elements have been determined experimentally by several laboratories, the absolute value of the contribution of oxygen to the molecular stopping cross section of the solid oxides can be evaluated by using the ratios in Table III and the reported stopping cross sections of the pure metals. The results of these calculations, using the selected values of the pure-metal stopping cross sections given in Table V, are shown in Table VI with the value reported for molecular O_2 in gas phase included for comparison. The stopping cross sections thus obtained are systematically (6–22)% lower than in gas phase.

V. DISCUSSION

A. Bragg additivity

The present results demonstrate that for these five oxides, there is a unique set of five stopping cross sections that is consistent with all combinations of pure metals and their oxides. Since this experiment depends on the energy loss of both the incoming and outgoing trajectories, this result is applicable to ^4He ions with energies of 1–2 MeV.

The compounds used in this study are the stoichiometric oxides with the lightest cations from

TABLE III. Relative stopping cross section of solid oxygen. The ratio of the stopping cross sections of "solid O_2 " and the metal were calculated from the yield ratios given in Table I using the procedure outlined in the text. The uncertainties in the values shown in parentheses were calculated by propagating the standard deviations shown in Table I.

Cation	Mg	Al	Si	Fe
$\frac{\epsilon_{\text{O}_2}^{\text{solid}}}{\epsilon_{\text{cation}}}$ at 2.0 MeV	1.34	1.33	1.36	0.90
	(3%)	(2%)	(1½%)	(2%)

TABLE IV. Relative oxygen stopping cross sections. This shows the variation in the contribution of oxygen to the stopping in the five oxides. These have been calculated by using the measured relative stopping cross sections as shown as Tables II and III. The values have been normalized to an average value of unity to emphasize the existence of a unique contribution to the molecular stopping cross section by the oxygen. The uncertainty in each value was calculated by propagating the standard deviations in the original measurements shown in Table I.

Oxide	MgO	Al_2O_3	SiO_2	$\alpha\text{-Fe}_2\text{O}_3$ Fe_2O_4
$\frac{\epsilon_{\text{oxygen}}^{2.0 \text{ MeV}}}{\langle \epsilon_{\text{oxygen}}^{2.0 \text{ MeV}} \rangle_{\text{av}}}$	0.995	0.989	1.016	0.999
	(3.4%)	(2.4%)	(2.0%)	(2.3%)

which the nuclear scattering at 2 MeV is purely electrostatic. This maximizes the fraction of valence-band electrons, which varies from 30 to 53%. A simple test of the nature of the chemical binding is the difference in Pauling electronegativity, which varies from 1.7 for Si-O to 2.3 for Mg-O. This covers almost the full range available for binary solid oxides. The estimated ionic character of the bonding of these oxides varies from 51 to 74%. Any changes in the stopping power due to chemical binding effects should be maximized by this choice of compounds. The present results indicate that there are no observable chemical effects in the stopping of 1–2-MeV ^4He ions by these solid oxides.

We expect that the present results can be extended to all other solid oxides and that the contribution of oxygen to the stopping in those oxides is independent of the choice of the cation.

B. Physical state effect

The reduction in the stopping cross section with increasing density due to dielectric effects was first recognized by Swann.¹² These effects have been shown to be large and easily observed for relativistic ion velocities in which Čerenkov radiation contributes to the loss of energy.¹³ By including these dielectric screening corrections for

TABLE V. Reference stopping cross sections (in $10^{-15}\text{eV}/\text{cm}^2$).

Element	O_2	Mg	Al	Si	Fe
ϵ (1.0 MeV)	94	56	52	67	93
ϵ (1.5 MeV)	83	50	47	58	85
ϵ (2.0 MeV)	72	44	42	49	75
Ref.	22	21	21	16	21

nonrelativistic particles, Fermi has estimated that the stopping in a condensed medium is "of the order of several percent" lower than in a gaseous medium.¹⁴ A recent calculation based on Lindhard and Winther's statistical approach has shown that, in addition, solid-state charge distributions produce lower stopping cross sections than Hartree-Fock-Slater wave functions for isolated atoms.¹⁵

In the energy range 0–2-MeV ⁴He ions, the most extensive experiments have been performed by the Baylor group. Their measurements on several hydrocarbon gases showed that the contribution to the stopping by the carbon in these compounds was systematically higher than the measured stopping power of solid carbon.² However, the carbon contribution to the stopping in fluorocarbon gases was found to be in good agreement with solid carbon.⁴

The systematic discrepancy observed in Table VI between the oxygen contribution in the solid oxides and in molecular oxygen is presented as possible evidence for a physical state effect. Because of the potential errors in the absolute stopping cross sections, each individual determination of the effective stopping cross section of solid oxygen by this method could not be construed as proof of the existence of a physical state effect. However, a systematic discrepancy is observed for all possible choices of reference stopping cross section. We discuss the effects of using other reference values below.

For example, the stopping in Si has been measured independently by three groups with good agreement between 1 and 2 MeV.^{16–18} We have used the values by Eisen *et al.*,¹⁶ the largest reported values. Using the other values would increase the apparent physical state effect by (2–5)%, giving values of (9–12)%, for this effect in SiO₂.

The Al stopping cross section has been reported

TABLE VI. Calculated absolute values for the stopping cross section of solid oxygen. The absolute values of the oxygen stopping cross section, calculated from the ratios shown in Table III and the values shown in Table VI, show a systematic deviation from the reported value for gaseous O₂, which is included for comparison.

Cation	Mg	Al	Si	Fe	O ₂ (gas)
$2 \times \epsilon_0^{\text{solid}}$ at 2.0 MeV (10^{-15} eV cm ²)	59	56	67	67	72
difference from gaseous O ₂	-18%	-22%	-7%	-6%	...

by several groups with agreement within about 5% for 1–2-MeV α particles. Because of the large inconsistencies in the Al-Si relative yields with respect to the reported stopping powers,⁸ we have recently remeasured the Al stopping cross section.¹⁹ These values are in good agreement with the results of Porat and Ramavataram,²⁰ which are (2–6)% higher than the results of Chu and Powers²¹ between 1 and 2 MeV. This would reduce the observed physical effect in Al₂O₃ from the 22% shown in Table VI to about 17%.

We have also remeasured the Fe stopping cross section¹⁹ and found slightly lower [(7±5)%] values than reported by Chu and Powers.²¹ This value would increase the apparent physical state effect in the two iron oxides to about 13%.

Bourland *et al.* directly measured the stopping cross section in gaseous oxygen,²² while Rotondi differentiated the range-energy relation.²³ These two measurements agree between 1.5 and 2 MeV with Rotondi's value about 5% higher at 1 MeV. Adopting Rotondi's data would increase the apparent physical state effect by (0–3)%, depending on the oxide.

By taking appropriate choices of reference data, the apparent physical state effect can be narrowed to about (10–15)%. This is almost exactly the value recently predicted by Ziegler and Chu.²⁴

The observed systematic discrepancy could also be attributed to chemical binding effects. The magnitude of these effects on the stopping in gaseous oxides can be estimated by considering the cases of N₂O, CO, and CO₂. Using the measurements of Bourland, Chu, and Powers²² of these gases as well as N₂ and O₂, it is possible to compare the contribution of oxygen to the stopping cross sections of the gaseous compounds with the stopping cross section of pure oxygen. In one case, CO and CO₂, there is no significant difference from pure oxygen for 1–2-MeV α particles. In the other case, N₂ and N₂O, the Bragg rule contribution of the oxygen is systematically (5–8)% lower than the pure oxygen value in the same energy range.

The existence of the apparent physical state effect assumes the accuracy of the referenced stopping-cross-section data. In addition, we have implicitly assumed that chemical effects are small. This produced the Bragg-rule assumption that the stopping power of atomic oxygen is one-half that of molecular oxygen. Because the existence of the apparent physical state effect depends crucially on these assumptions, the data have been presented in a form that allows including any new values of the stopping powers to continually test the possibility that there may be a physical state effect for oxygen.

C. Stopping-cross-section values

The stopping-cross-section ratios found in this work, e.g., Table II, can be used to critically select a set of preferred stopping-cross-section values for Mg, Al, Si, and Fe. For example, using the values for Si reported by Lin, Olsen, and Powers¹⁷ and the data of Porat and Ramavataram²⁰ for Al would significantly reduce the discrepancy between the reported absolute stopping cross sections and our measured yield ratios. This also suggests that the stopping cross section of Mg should be about (5–10)% higher than the value reported by Chu and Powers, while the Fe values should be reduced by (5–10)%.

We also note that the experimental techniques involved in absolute measurements of the stopping cross section in gaseous and condensed media are very different. This suggests that the observed physical state effects may arise from systematic discrepancies in the analysis of the data taken by the two methods. We regard this as highly improbable.

VI. CONCLUSIONS

We have described a self-consistent procedure for testing Bragg's rule that does not require the knowledge of any absolute stopping-cross-section

values. This has been used to demonstrate that the contribution of oxygen to the stopping of 1–2-MeV ⁴He ions in oxides is independent of the cation element. This is an important necessary condition for applying Bragg additivity of stopping cross sections to these compounds.

Although the method of testing Bragg's rule described here has been applied only to oxides, it can obviously be extended to all stoichiometric solid compounds. It is most useful for testing binary compound systems such as oxides or nitrides (Si₃N₄-AlN-BN), in which the normal phase of the one element common to all the compounds is not normally a solid. It can also be extended to test the reproducibility of the stopping cross sections of chemical radicals such as (NO₃)⁻, (SO₄)⁻⁻, etc. The advantage of this test is that in its self-consistency or in its failure to achieve self-consistency, it does not depend on any absolute measurements.

Completing the test of Bragg additivity requires a demonstration of the equality of the oxygen stopping cross sections in solid phase and in gas phase. By using the reported values of the absolute stopping cross sections of the metals used in this study, it is found that the calculated contribution of oxygen to the molecular stopping cross section is systematically (6–22)% lower in the solid oxides than in gas-phase O₂.

*Work supported in part by Office of Naval Research (L. Cooper).

¹W. H. Bragg and R. Kleeman, *Philos. Mag.* **10**, S318 (1905).

²P. D. Bourland and D. Powers, *Phys. Rev. B* **3**, 3635 (1971).

³D. Powers, A. S. Lodhi, W. K. Lin, and H. L. Cox, *Thin Solid Films* **19**, 205 (1973).

⁴D. Powers, W. K. Chu, R. J. Robinson, and A. S. Lodhi, *Phys. Rev. A* **6**, 1425 (1972).

⁵M.-A. Nicolet, J. W. Mayer, and I. V. Mitchell, *Science* **177**, 841 (1972).

⁶D. A. Thompson and W. D. Mackintosh, *J. Appl. Phys.* **42**, 3969 (1971).

⁷J. S.-Y. Feng, W. K. Chu, and M.-A. Nicolet, *Thin Solid Films* **19**, 227 (1973).

⁸J. S.-Y. Feng, W. K. Chu, J. W. Mayer, and M.-A. Nicolet, *Thin Solid Films* **19**, 195 (1973).

⁹J. E. E. Baglin and J. F. Ziegler, *J. Appl. Phys.* **45**, 1413 (1974).

¹⁰C. G. Darwin, *Philos. Mag.* **28**, 499 (1914).

¹¹J. F. Ziegler and W. K. Chu, IBM Res. Rept. No. RC

4288 (No. 19193), 1973 (unpublished).

¹²W. F. G. Swann, *J. Franklin Inst.* **226**, 598 (1938).

¹³A recent review on this subject can be found in A. Crispin and G. N. Fowler, *Rev. Mod. Phys.* **42**, 290 (1970).

¹⁴E. Fermi, *Phys. Rev.* **57**, 485 (1940).

¹⁵W. K. Chu, V. L. Moruzzi, and J. F. Ziegler (unpublished).

¹⁶F. H. Eisen, C. J. Clark, J. Böttiger, and J. M. Poate, *Radiat. Eff.* **13**, 93 (1972).

¹⁷W. K. Lin, H. G. Olsen, and D. Powers, *J. Appl. Phys.* **44**, 3631 (1973).

¹⁸J. F. Ziegler and M. H. Brodsky, *J. Appl. Phys.* **44**, 188 (1973).

¹⁹J. S.-Y. Feng (unpublished).

²⁰D. I. Porat and K. Ramavataram, *Proc. Phys. Soc. Lond.* **78**, 1135 (1961).

²¹W. K. Chu and D. Powers, *Phys. Rev.* **187**, 478 (1969).

²²P. D. Bourland, W. K. Chu, and D. Powers, *Phys. Rev. B* **3**, 3625 (1971).

²³E. Rotondi, *Radiat. Res.* **33**, 1 (1968).

²⁴J. F. Ziegler and W. K. Chu (unpublished).

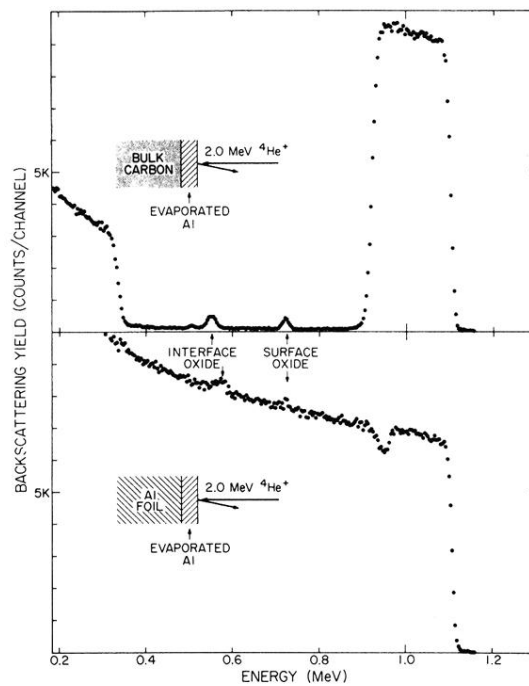


FIG. 1. Purity tests of Al films. The top half of the figure shows a back-scattering spectrum of Al evaporated onto a carbon substrate. This shows the presence of a small amount of oxygen on the two surfaces of the film, but no evidence of bulk impurities. The bottom part shows the spectrum of Al evaporated onto Al foil. The dip in the yield near 975 keV is due to the native oxide on the Al foil. The match in the yields of the evaporated and bulk Al indicates that there are no significant undetected impurities.